Accelerated Destructive Degradation Test Planning

Ying Shi
Dept. of Statistics
Iowa State University
Ames, IA 50011
yshi@iastate.edu

Luis A. Escobar
Dept. of Experimental Statistics
Louisiana State University
Baton Rouge, LA 70803
luis@lsu.edu

William Q. Meeker
Dept. of Statistics
Iowa State University
Ames, IA 50011
wqmeeker@iastate.edu

Abstract

Accelerated Destructive Degradation Tests (ADDTs) provide reliability information quickly. An ADDT plan specifies factor level combinations of an accelerating variable (e.g., temperature) and evaluation time and the allocations of test units to these combinations. This paper describes methods to find good ADDT plans for an important class of destructive degradation models. First, a collection of optimum plans is derived. These plans minimize the large sample approximate variance of the maximum likelihood (ML) estimator of a specified failure-time quantile. The General Equivalence Theorem (GET) is used to verify the optimality of these plans. Because an optimum plan is not robust to the model specification and the planning information used in deriving the plan, a more robust and useful compromise plan is proposed. Sensitivity analyses show the effects that changes in sample size, time duration of the experiment, levels of the accelerating variable, and misspecification of the planning information have on the precision of the ML estimator of a quantile of the failure-time distribution. Monte Carlo simulations are used to evaluate the statistical characteristics of the ADDT plans. The methods are illustrated with an application for an adhesive bond.

KEY WORDS: reliability, large sample approximate variance, optimum ADDT plan, general equivalence theorem, compromise ADDT plan, Monte Carlo simulation.

1 Introduction

1.1 Motivation

Manufacturers often conduct up-front reliability tests on materials and components when their products are being designed. Because degradation data provide more information on reliability than traditional failure-time data (where time to failure is the response), especially in applications where few or no failures are expected, degradation tests are used in manufacturing industries to obtain reliability information of product components and materials. For most applications, however, degradation rates at normal use conditions are so low that appreciable degradation will not be observed in a test of practical time length. For this reason, degradation tests are often accelerated to get reliability information more quickly. Generally, information from tests at high levels of accelerating variables is extrapolated to obtain estimates of lifetime or degradation rates at lower, normal use conditions based on a physically reasonable statistical model.

1.2 Accelerated Destructive Degradation Test

For some applications, the degradation measurement process destroys or changes the physical/mechanical characteristics of test units so that only one meaningful measurement can be taken on each unit. An accelerated degradation test with such degradation data is called an "accelerated destructive degradation test" or ADDT.

Escobar, Meeker, Kugler, and Kramer (2003) described an application of an accelerated destructive degradation test to evaluate an adhesive bond (Adhesive Bond B). The response was the strength (in Newtons) of the adhesive bond over time. The measurement process was destructive because the strength of test unit could only be measured once. Additionally, there was special interest in estimating the time at which 1% of the devices would have a strength below 40 Newtons when operating at room temperature of 25 °C (i.e., the 0.01 quantile of the failure-time distribution). To obtain information about the 0.01 quantile of the failure-time distribution, an accelerated destructive degradation test was used. As a baseline, 8 units with no aging were measured at the start of the experiment. A total of 80 additional units were aged and measured according to the temperature and time schedule presented in Table 1.

Table 1: Original ADDT Plan

Temperature °C	Weeks 0	2	4	6	12	16	Totals
—	8						8
50		8	0	8	8	7	31
60		6	0	6	6	6	24
70		6	6	4	9	0	25
Totals	8	20	6	18	23	13	88

1.3 Related Literature

Nelson (1981) and Nelson (1990, chapter 11) introduced basic models and methods for analyzing ADDT data. Escobar, Meeker, Kugler, and Kramer (2003) provided an application for accelerated destructive degradation data and introduced a more general class of models. There is a large amount of literature on planning accelerated tests. This work has been summarized by Nelson (2005a, 2005b). Some work that is particularly relevant to this paper is included in the following references. Nelson (1990, Chapter 6) described methods for planning accelerated life tests (ALTs) based on a simple model. Meeker and Escobar (1998, chapter 20) provided details and examples on how to plan a single-variable ALT. Escobar and Meeker (1995) described methods for planning ALT's with two or more variables. There are some important differences between accelerated life tests and accelerated degradation tests. The most important difference is that ALTs almost always result in censored data. Censoring is not as common in ADDTs. Boulanger and Escobar (1994) proposed methods for planning *repeated measures* accelerated degradation tests. In this paper, we use the application in Escobar, Meeker, Kugler, and Kramer (2003) and describe methods for planning accelerated destructive degradation tests.

1.4 Overview

The remainder of this paper is organized as follows. Section 2 presents a class of models for ADDT data and gives formulas for the degradation distribution. Section 3 gives formulas for the failure-time distribution induced by the degradation models. Section 4 outlines the framework for accelerated destructive degradation test planning. Section 5 gives optimum ADDT plans and applies the general equivalence theorem (GET) to verify the optimality of test plans. Section 6 describes alternative ADDT plans and compares the results of different test plans. Section 7 illustrates the effects of

changing constraints and investigates sensitivity to misspecification of the planning information. Section 8 uses Monte Carlo simulation to evaluate different test plans. Section 9 contains some concluding remarks and extensions for future research work. Appendix A provides derivations and technical details about large sample approximations that are used to evaluate ADDT plans. Appendix B verifies that the ADDT planning problem satisfies the necessary conditions for using the GET.

2 Degradation Models

2.1 Accelerated Degradation Models

The degradation level for a typical observational unit at time t and accelerating variable AccVar (e.g., temperature, humidity) is denoted by $\mathcal{D}(\tau, x, \boldsymbol{\beta})$, where $\tau = h_t(t)$ and $x = h_a(\text{AccVar})$ are known monotone increasing transformations of t and AccVar respectively, and $\boldsymbol{\beta}$ is a vector of unknown parameters.

For the class of degradation models used here, transformed degradation Y for a unit at transformed time τ and transformed accelerating variable level x is

$$\begin{aligned} Y &= \mu(\tau, x) + \epsilon \\ &= \beta_0 + \beta_1 \exp(\beta_2 x)\tau + \epsilon \end{aligned} \tag{1}$$

where $\mu(\tau, x) = h_d(\mathcal{D})$ is a monotone increasing transformation of $\mathcal{D}$ and $\mu(\tau, x)$ is a location parameter for the distribution of Y that depends on the unknown parameters in $\boldsymbol{\beta} = (\beta_0, \beta_1, \beta_2)$. ϵ is a residual deviation that describes unit-to-unit variability with $(\epsilon/\sigma) \sim \Phi(z)$, where $\Phi(z)$ is a completely specified cdf. For example, $\Phi(z)$ can be replaced by $\Phi_{\text{nor}}(z)$, the standardized normal cdf, or $\Phi_{\text{sev}}(z)$, the standardized smallest extreme value cdf. The model parameters $\boldsymbol{\beta}$ and σ are fixed but unknown.

Model (1) is linear in the sense that for specified x, the mean transformed degradation path $\mu(\tau, x)$ is linear in τ. For purposes of estimation, however, the model in (1) is nonlinear in the parameters. β_0 is the location parameter of the transformed degradation when $\tau = 0$. The degradation rate of $\mu(\tau, x)$ with respect to τ at x is $\omega(x) = \beta_1 \exp(\beta_2 x)$. The sign of β_1 determines whether the degradation is increasing or decreasing over time. For example if the degradation response is size

of a crack or the concentration of a harmful material, β_1 would be expected to be positive. On the other hand, if the degradation response is light output of a LED or the strength of an adhesive bond, β_1 would be negative.

For the Adhesive Bond B application, the strength degradation model used in Escobar, Meeker, Kugler, and Kramer (2003) is as given in (1) with

$$\begin{aligned} Y &= h_d(\text{Strength}) = \log(\text{Strength in Newtons}) \\ \tau &= h_t(\text{Time}) = \sqrt{\text{Time in Weeks}} \\ x &= h_a(\text{Temperature}) = -\frac{11604.83}{\text{Temperature in } ^\circ\text{C} + 273.15} \\ (\epsilon/\sigma) &\sim \Phi_{\text{nor}}(z). \end{aligned}$$

The accelerating variable for this application is temperature. The denominator in x is temperature on the kelvin (K) scale and the numerator is the reciprocal of Boltzmann's constant in units of electronvolt per kelvin (eV/K). For this parametrization, β_2 has the interpretation of an effective activation energy.

2.2 Degradation CDF

For given time and accelerating variable level, the CDF for the transformed degradation Y is

$$F_Y(y;\tau,x) = \Pr(Y \le y;\tau,x) = \Phi\left[\frac{y-\mu(\tau,x)}{\sigma}\right]$$

where $\mu(\tau,x) = \beta_0 + \beta_1 \exp(\beta_2 x)\tau$.

For the Adhesive Bond B example, the CDF of $F_Y(y;\tau,x)$ at a fixed factor level combination of time and temperature can be obtained by replacing Φ with Φ_{nor}. Figure 1 shows the degradation distributions at 25 °C and different values of time for particular values of the parameters $\beta_0, \beta_1, \beta_2, \sigma$ corresponding to the maximum likelihood (ML) estimates given in Escobar, Meeker, Kugler, and Kramer (2003).

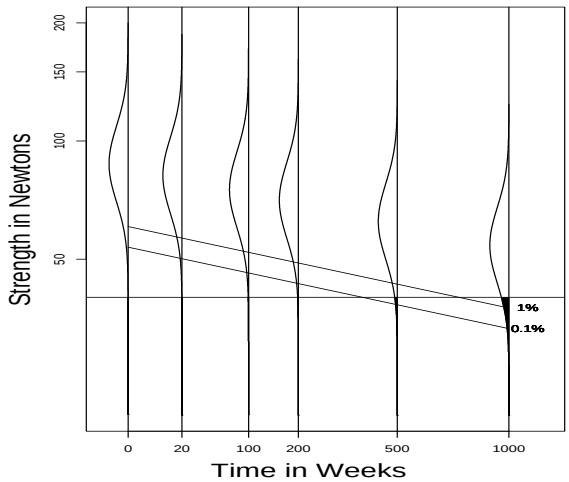

Figure 1: Adhesive Bond B degradation distributions as a function of time at 25 °C. The strength axis is a logarithmic axis and the time axis is a square root axis. The horizontal line at $\mathcal{D}_{\mathrm{f}} = 40$ Newtons is the failure-definition degradation level. At each time t, the shaded area below the horizontal line is the failure probability at t.

2.3 Degradation Quantiles

The p quantile function for the transformed degradation at (τ, x) is

$$\begin{aligned} y_p &= \mu(\tau, x) + \sigma\Phi^{-1}(p) \\ &= \beta_0 + \beta_1 \exp(\beta_2 x)\tau + \sigma\Phi^{-1}(p) \end{aligned}$$

where $\Phi^{-1}(p)$ is the p quantile of the standard location-scale distribution.

Substituting $\Phi^{-1}_{\mathrm{nor}}(p)$ for $\Phi^{-1}(p)$, one obtains the p quantile for the transformed degradation (log Newtons) for the Adhesive Bond B example, such as the 0.01 and 0.001 quantiles shown in Figure 1.

3 Failure-Time Distribution for Degradation Models

3.1 Relationship Between Degradation and Failure

For some products, there is a gradual loss of performance with increasing time (e.g., decreasing strength of an adhesive bond). Then failure would be defined at a specified degradation level. This failure-definition is known as a "soft failure" (see Chapter 13 of Meeker and Escobar 1998). We use

$\mathcal{D}_{\mathrm{f}}$ to denote the critical level for the degradation distribution at which failure is assumed to occur. The failure-time T is defined as the time when the observed degradation crosses the critical level $\mathcal{D}_{\mathrm{f}}$.

3.2 Failure-Time CDF

As mentioned in Section 2.1, degradation can be decreasing or increasing over time, depending on the sign of β_1. For decreasing degradation (i.e., when β_1 is negative), failure-time T being less than t is equivalent to an observed degradation being less than the critical level $\mathcal{D}_{\mathrm{f}}$ at time t (i.e., the event $T \leq t$ is equivalent to the event $Y \leq y_{\mathrm{f}}$, where $y_{\mathrm{f}} = h_d(\mathcal{D}_{\mathrm{f}})$), as illustrated in Figure 1. Then the failure-time CDF is

$$\begin{aligned} F_T(t;x) &= \Pr(T \leq t) = \Pr(Y \leq y_{\mathrm{f}}) = F_Y(y_{\mathrm{f}};\tau,x) \\ &= \Phi\left[\frac{y_{\mathrm{f}} - \mu(\tau,x)}{\sigma}\right] = \Phi\left(\frac{\tau-\nu}{\varsigma}\right), \quad \text{for } t \geq 0 \end{aligned} \tag{2}$$

where

$$\nu = \frac{(\beta_0 - y_{\mathrm{f}})\exp(-\beta_2 x)}{\mid \beta_1 \mid} \quad \text{and} \quad \varsigma = \frac{\sigma \exp(-\beta_2 x)}{\mid \beta_1 \mid}.$$

With a time transformation $h_t(t)$ for which $\tau = 0$ when $t = 0$, the failure-time distribution for decreasing degradation is a mixture with a spike $\Pr(T = 0) = \Phi\left[(y_{\mathrm{f}} - \beta_0)/\sigma\right] = \Phi\left(-\nu/\varsigma\right)$ at $t = 0$. This spike represents the probability of failure for a new unit that experiences no aging and is sometimes called the dead-on-arrival (or DOA) probability. For $t > 0$ the cdf of failure-time in (2) is continuous and it agrees with the cdf of a log-location-scale variable with standardized cdf $\Phi(\cdot)$, location parameter ν and scale parameter ς.

For increasing degradation (i.e., β_1 is positive), failure-time T being less than t is equivalent to an observed degradation being greater than the critical level $\mathcal{D}_{\mathrm{f}}$ at time t (i.e., the event $T \leq t$ is equivalent to the event $Y \geq y_{\mathrm{f}}$, where $y_{\mathrm{f}} = h_d(\mathcal{D}_{\mathrm{f}})$). Then

$$\begin{aligned} F_T(t;x) &= \Pr(T \leq t) = \Pr(Y \geq y_{\mathrm{f}}) = 1 - F_Y(y_{\mathrm{f}};\tau,x) \\ &= 1 - \Phi\left[\frac{y_{\mathrm{f}} - \mu(\tau,x)}{\sigma}\right] = 1 - \Phi\left(\frac{-\tau-\nu}{\varsigma}\right), \quad \text{for } t \geq 0. \end{aligned} \tag{3}$$

In this case the spike at $t = 0$ is $\Pr(T = 0) = 1 - \Phi\left[(y_{\mathrm{f}} - \beta_0)/\sigma\right] = 1 - \Phi\left(-\nu/\varsigma\right)$.

3.3 Failure-Time Quantiles

From (2), the p quantile of the failure-time for decreasing degradation is

$$t_p = \begin{cases} h_t^{-1}\left[\nu + \varsigma\Phi^{-1}(p)\right] & \text{if } p \geq \Phi\left(-\nu/\varsigma\right) \\ 0 & \text{otherwise.} \end{cases}$$

From (3), the p quantile of the failure-time for increasing degradation is

$$t_p = \begin{cases} h_t^{-1}\left\{-\left[\nu + \varsigma\Phi^{-1}(1-p)\right]\right\} & \text{if } p \geq 1 - \Phi\left(-\nu/\varsigma\right) \\ 0 & \text{otherwise.} \end{cases}$$

In both cases, ν and ς are as defined in Section 3.2.

4 Accelerated Destructive Degradation Test Planning

4.1 ADDT Planning Information

ADDT planning requires information that includes planning values for the model parameters, a plausible distribution for the model variability, a specification of the critical degradation level, the range of accelerating variable available for experiment. There will also be constraints on the maximum test time and the number of units available for testing.

For the Adhesive Bond B example, the degradation model is described in Section 2.1. The critical degradation level is specified as $\mathcal{D}_{\mathrm{f}} = 40$ Newtons. Some constraints for this application are:

- 88 test units.
- 70 °C is the maximum temperature that can be used (higher temperatures would cause the model to breakdown).
- 16 weeks are available for testing.

The goal is to develop a test plan to evaluate a new adhesive bond material similar to the material used in the example described in Escobar, Meeker, Kugler, and Kramer (2003). Test plan properties will depend on the unknown parameters $\boldsymbol{\theta} = (\beta_0, \beta_1, \beta_2, \sigma)'$. The planning values of the parameters are $\beta_0^{\square} = 4.471$, $\beta_1^{\square} = -864064160$, $\beta_2^{\square} = 0.6364$, and $\sigma^{\square} = 0.1580$. These values derive from the

data analysis in Escobar, Meeker, Kugler, and Kramer (2003). The planning information defines the mean transformed degradation paths $\mu(\tau, x)$ at all levels of temperature and the degradation distribution at a given factor level combination of time and temperature, as depicted in Figure 2. Note that the strength axis is a logarithmic axis and that the time axis is a square root axis so that the mean transformed degradation paths are linear with respect to the transformed time.

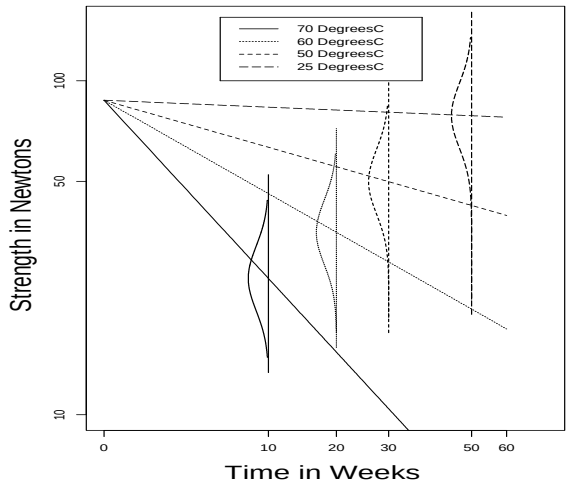

Figure 2: Model for degradation evaluated at four different temperatures. The lines for each temperature indicate mean transformed degradation paths $\mu(\tau, x)$ as a function of time.

An alternative specification of the planning values is to give the degradation rate (slope of the line), $\omega^{\square}$, of $\mu(\tau, x)$ for a given temperature, say $\omega^{\square} = -0.1026$ at 50 °C instead of $\beta_1^{\square}$. This method has the advantage that each of the model parameters has a clear practical interpretation, making it easier to elicit from experts when needed. With this specification at 50 °C, one gets

$$\beta_1^{\square} = \omega^{\square} \exp(-\beta_2^{\square} x) = -0.1026 \exp(0.6364 \times 35.9116) = -864122323$$

where $x = -11604.83/(50\ ^\circ\mathrm{C} + 273.15) = -35.9116$. The difference in the values for $\beta_1^{\square}$ obtained from the two methods is due to rounding in the specifications of $\omega^{\square}$ and $\beta_2^{\square}$.

4.2 ADDT Plan Specification

Denote a factor level combination of transformed time τ and transformed accelerating variable x as $\boldsymbol{v} = (\tau, x)$. An ADDT plan will specify a set of factor level combinations $\boldsymbol{v}_i$ and the corresponding

proportional allocation π_i of test units at $\boldsymbol{v}_i$. A test plan with r factor level combinations is denoted as

$$\boldsymbol{\xi} = \begin{bmatrix} \boldsymbol{v}_1, & \pi_1 \\ \boldsymbol{v}_2, & \pi_2 \\ \vdots & \vdots \\ \boldsymbol{v}_r, & \pi_r \end{bmatrix}$$

where $\pi_i > 0$ and $\sum_{i=1}^{r} \pi_i = 1$.

4.3 Criterion for Choosing ADDT Plans

The appropriate criterion for planning an ADDT depends on the purpose of the experiment. For accelerated tests, a common objective is to estimate a particular quantile of the failure-time distribution at use conditions, say, t_p. For this reason, a commonly used criterion for planning accelerated tests is to minimize $\text{Avar}(\widehat{t_p})$, the large sample approximate variance of the maximum likelihood (ML) estimator of the specified failure-time quantile. We use this criterion in our work. Because $h_t(t_p)$ is a monotone function of t_p, minimizing $\text{Avar}[h_t(\widehat{t_p})]$ gives the same test plan as minimizing $\text{Avar}(\widehat{t_p})$.

As explained in Appendix A.3, the optimization criterion is equivalent to finding the test plan $\boldsymbol{\xi}$ that maximizes the objective function

$$\Psi[\mathcal{I}(\boldsymbol{\xi})] = -\boldsymbol{c}'[\mathcal{I}(\boldsymbol{\xi})]^{-1}\boldsymbol{c} \tag{4}$$

where $\boldsymbol{c} = \partial h_t(t_p)/\partial\boldsymbol{\theta}, \boldsymbol{\theta} = (\beta_0, \beta_1, \beta_2, \sigma)'$, and $\mathcal{I}(\boldsymbol{\xi})$ is the scaled information matrix of the model parameters. This criterion is closely related to C optimality (see Pukelsheim 1993). Details are given in Appendix A.

5 Optimum ADDT Plan

5.1 Optimum ADDT Plan Structure

The degradation model described in (1) has three regression parameters. This suggests that a non-degenerate optimum ADDT plan for an application with this degradation model should be a 3-point plan (i.e., the test plan should have three factor level combinations). For most practical situations in which accelerated tests are used, an optimum plan will allocate test units on the boundaries of the experimental region. To minimize the large sample approximate variance for the ML estimator of a specified quantity, an optimum ADDT plan should spread the three factor level combinations as much as possible, providing better estimates of the regression coefficients than closely-spaced test conditions. Figure 3 presents an ADDT optimum plan structure in terms of the experimental variables τ and x. Under the practical constraints of a maximum transformed time τ_{M} and a maximum transformed accelerating variable level x_{M}, one particular optimum plan will have some test units allocated at $\boldsymbol{v}_1^*$ (baseline test condition) with $\tau = 0$, some at the $\boldsymbol{v}_2^*$ test condition with τ_{M} and x_{M}, and some at the $\boldsymbol{v}_3^*$ test condition with τ_{M} and an optimized value x^*. The x^* for the $\boldsymbol{v}_3^*$ test condition and the proportional allocations π_1^*, π_2^* of test units are chosen to optimize the plan. Note that $\pi_3^* = 1 - \pi_1^* - \pi_2^*$ and the degradation model at $\tau = 0$ (and thus test plan properties) does not depend on the level of x. Using notation similar to that used in Section 4.2, this particular optimum test plan is denoted by

$$\boldsymbol{\xi}^* = \begin{bmatrix} \boldsymbol{v}_1^*, & \pi_1^* \\ \boldsymbol{v}_2^*, & \pi_2^* \\ \boldsymbol{v}_3^*, & \pi_3^* \end{bmatrix} = \begin{bmatrix} (0, \bullet), & \pi_1^* \\ (\tau_{\mathrm{M}}, x_{\mathrm{M}}), & \pi_2^* \\ (\tau_{\mathrm{M}}, x^*), & \pi_3^* \end{bmatrix} \tag{5}$$

where $\bullet$ indicates that at $\tau = 0$, the level of x is arbitrary. In the next section a variation of Whittle's (1973) general equivalence theorem (GET) is used to verify the optimality of this test plan.

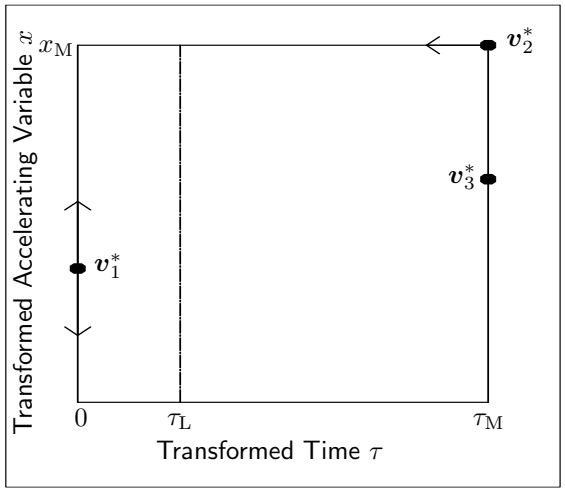

Figure 3: Optimum Plan Structure

5.2 Checking the Initial Optimum Plan

Here we check the optimality of the test plan $\boldsymbol{\xi}^*$ using the GET. The directional derivative, Λ, of Ψ at $\boldsymbol{\xi}$ and in the direction of an alternative plan $\boldsymbol{\eta}$ is defined as

$$\Lambda(\boldsymbol{\xi}, \boldsymbol{\eta}) = \lim_{\delta \to 0^+} \frac{\Psi[(1-\delta)\boldsymbol{\xi} + \delta\boldsymbol{\eta}] - \Psi(\boldsymbol{\xi})}{\delta}.$$

As shown in Appendix B.1, $\Lambda(\boldsymbol{\xi}, \boldsymbol{\eta}) = \boldsymbol{c}'[\mathcal{I}(\boldsymbol{\xi})]^{-1}\mathcal{I}(\boldsymbol{\eta})[\mathcal{I}(\boldsymbol{\xi})]^{-1}\,\boldsymbol{c} - \boldsymbol{c}'\,[\mathcal{I}(\boldsymbol{\xi})]^{-1}\,\boldsymbol{c}$, where $\boldsymbol{c}$, $\mathcal{I}(\boldsymbol{\xi})$, and $\mathcal{I}(\boldsymbol{\eta})$ are evaluated at the planning values. Let $\boldsymbol{\xi}_{\boldsymbol{v}}$ be a singular test plan that puts all units at the $\boldsymbol{v}$ test condition. From the results in Appendix B.1, the plan $\boldsymbol{\xi}^*$ is an optimum plan if it satisfies $\Lambda(\boldsymbol{\xi}^*, \boldsymbol{\xi}_{\boldsymbol{v}_1^*}) = \Lambda(\boldsymbol{\xi}^*, \boldsymbol{\xi}_{\boldsymbol{v}_2^*}) = \Lambda(\boldsymbol{\xi}^*, \boldsymbol{\xi}_{\boldsymbol{v}_3^*}) = 0$ and $\Lambda(\boldsymbol{\xi}^*, \boldsymbol{\xi}_{\boldsymbol{v}}) \leq 0$ for any singular plan $\boldsymbol{\xi}_{\boldsymbol{v}}$ in the experimental region.

For the Adhesive Bond B application, a particular optimum plan (obtained numerically) is

$$\boldsymbol{\xi}^* = \begin{bmatrix} (0, \bullet), & \pi_1^* \\ (\tau_{\mathrm{M}}, x_{\mathrm{M}}), & \pi_2^* \\ (\tau_{\mathrm{M}}, x^*), & \pi_3^* \end{bmatrix} = \begin{bmatrix} (0, \bullet), & 0.20374 \\ (4, -33.819), & 0.16160 \\ (4, -35.390), & 0.63466 \end{bmatrix} \tag{6}$$

where -33.819 and -35.390 are the transformed temperatures corresponding to the maximum 70 °C and optimized 54.764 °C, respectively. In terms of the the original variables (Weeks and °C), this

plan is shown in Table 2.

Table 2: Initial Optimum Plan. The • indicates that at time 0, the level of temperature is arbitrary.

Optimum Test Condition	Weeks	Temperature °C	Proportional Allocations
$\boldsymbol{v}_1^*$	0	•	0.20374
$\boldsymbol{v}_2^*$	16	70	0.16160
$\boldsymbol{v}_3^*$	16	54.764	0.63466

Figure 4 shows the directional derivatives $\Lambda(\boldsymbol{\xi}^*, \boldsymbol{\xi}_{\boldsymbol{v}})$ of this optimum plan as a function of temperature and time, where $\boldsymbol{\xi}_{\boldsymbol{v}}$ is a plan that puts all units at the $\boldsymbol{v}$ test condition. Observe that, as required, the directional derivatives are zero at the three test conditions of the optimum plan. Also, the directional derivatives are zero at all the test conditions with temperature equal to 70 °C. This suggests the existence of alternative optimum plans.

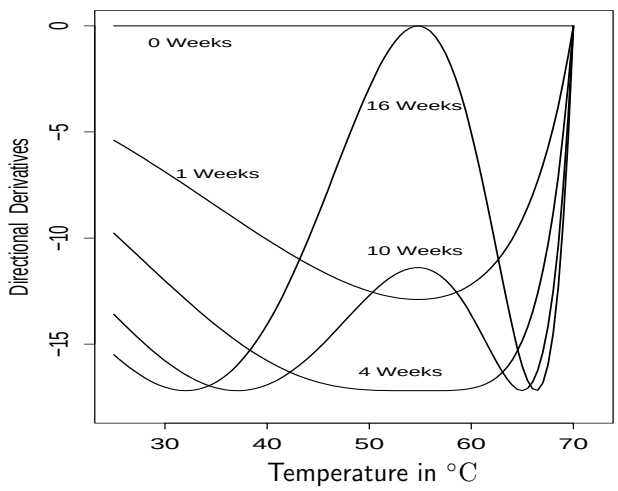

Figure 4: Directional derivatives $\Lambda(\boldsymbol{\xi}^*, \boldsymbol{\xi}_{\boldsymbol{v}})$ of the initial optimum plan as a function of temperature and time.

5.3 Alternative Optimum Plans

From Figure 4 and (20) in Appendix B.2, $\Lambda(\boldsymbol{\xi}^*, \boldsymbol{\xi}_{\boldsymbol{v}_2}) = 0$ where $\boldsymbol{\xi}_{\boldsymbol{v}_2}$ is a test plan putting all units at $\boldsymbol{v}_2 = (\tau, x_{\mathrm{M}})$, for all $0 \leq \tau \leq \tau_M$. This result suggests that we can move the $\boldsymbol{v}_2^*$ test condition to the left along the horizontal line with $x = x_{\mathrm{M}}$, as shown in Figure 3. Using the GET, it can be shown that, for fixed τ_a, $\tau_{\mathrm{L}} \leq \tau_a \leq \tau_{\mathrm{M}}$, and $\tau_{\mathrm{L}} = \tau_{\mathrm{M}}\pi_2^*/(\pi_1^* + \pi_2^*)$, an alternative optimum plan can

be expressed as

$$\boldsymbol{\xi}^a = \begin{bmatrix} \boldsymbol{v}_1 = (0, \bullet), & \pi_1 = \pi_1^* + \pi_2^* - \pi_2^* \dfrac{\tau_M}{\tau_a} \\ \boldsymbol{v}_2 = (\tau_a, x_{\mathrm{M}}), & \pi_2 = \pi_2^* \dfrac{\tau_M}{\tau_a} \\ \boldsymbol{v}_3 = (\tau_{\mathrm{M}}, x^*), & \pi_3 = \pi_3^* \end{bmatrix}. \tag{7}$$

See Appendix B.2 for the details.

For the Adhesive Bond B application, $\tau_L = 4\pi_2^*/(\pi_1^* + \pi_2^*) = 1.77$. The lower boundary of time for the $\boldsymbol{v}_2$ test condition in Weeks is $t_L = \tau_L^2 = 3.13$. A particular alternative optimum plan can be obtained by substituting the values $\tau_M = 4$, $x_M = -33.819$, $x^* = -35.390$, $\pi_1^* = 0.20374$, $\pi_2^* = 0.16160$, and $\pi_3^* = 0.63466$ from (6) into the expression (7) and choosing a value of τ_a, $1.77 \leq \tau_a \leq 4$. Figure 5 describes how the large sample approximate standard error of $\widehat{t}_{0.01}$ and the proportional allocations of test units change for different optimum plans as the time component of the $\boldsymbol{v}_2$ test condition varies in the experimental time range. Figure 5 illustrates the characteristics of the multiple optimum plans, the changing trend of proportional allocations of test units for different optimum plans, and the lower time bound t_L. Note that the directional derivatives in Figure 4 and the large sample approximate standard errors of $\widehat{t}_{0.01}$ in Figure 5 were computed for the continuous test plan with a sample size of 88 (a continuous test plan is one that has non-integer allocations because optimization was done without integer constraints on the number of units allocated to the test conditions).

Figure 5 and the results in (7) show that the optimized values of x and π_3 for the $\boldsymbol{v}_3$ test condition are the same for all optimum plans. However, as the value of τ_a for the $\boldsymbol{v}_2$ test condition increases, the π_1 increases and π_2 decreases, as shown in Figure 5. These results are not surprising because as the value of transformed time τ_a for the $\boldsymbol{v}_2$ test condition approaches τ_{L}, $\boldsymbol{v}_2$ provides information that is similar to the baseline $\boldsymbol{v}_1$ test condition. As the value of τ_a for $\boldsymbol{v}_2$ increases, the $\boldsymbol{v}_2$ test condition is further away from $\boldsymbol{v}_1$ so that more units are allocated to $\boldsymbol{v}_1$ to get more information about the degradation distribution. Also, when the value of transformed temperature x for the $\boldsymbol{v}_3$ test condition is too small, the information from $\boldsymbol{v}_3$ will be similar to that from $\boldsymbol{v}_1$ (i.e., both $\boldsymbol{v}_1$ and $\boldsymbol{v}_3$ behave like a unit tested at low temperature). When the value of x for $\boldsymbol{v}_3$ is too close to x_{M}, there will not be good information separating the effect that time and the accelerating variable have on the degradation rates. It is interesting that the optimized values of x for the $\boldsymbol{v}_3$ test condition

for different optimum plans are the same. Also, as τ_a approaches τ_{L} from above, the limiting plan is degenerate and will not allow estimation of all of the model parameters, even though it will allow estimation of the lifetime distribution at the use conditions. Of course, such "degenerate" test plans have little practical value.

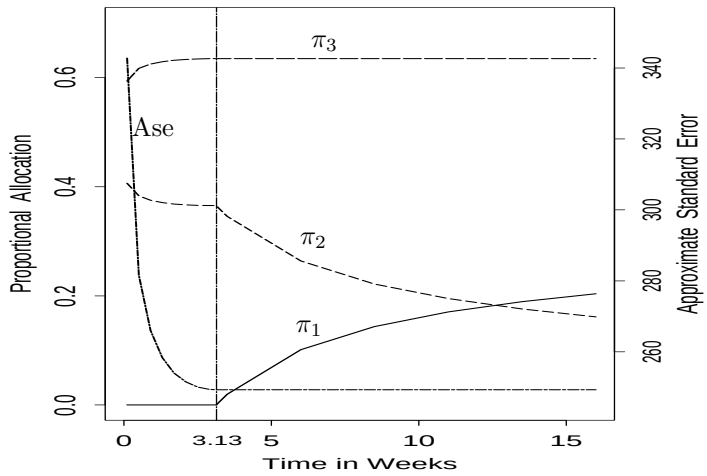

Figure 5: Proportional allocations and large sample approximate standard error of $\widehat{t}_{0.01}$ as a function of time in Weeks showing different optimum plans (Time $\geq$ 3.13 Weeks) and optimized plans (Time $<$ 3.13 Weeks) arising from the constraint $\pi_1 \geq 0$.

6 Other ADDT Plans

6.1 Traditional ADDT Plans

A traditional plan is one that uses equally-spaced levels of the experimental conditions and equal allocations to all factor level combinations. In applications involving extrapolation, like accelerated testing, such traditional plans may not be statistically efficient, which results in less precise estimates.

6.2 Motivation for Compromise ADDT Plans

An optimum plan provides the smallest large sample approximate variance of the maximum likelihood estimator of a specified quantity. Optimum plans, however, have practical deficiencies (e.g., only a small number of factor level combinations) and provide no information to check the adequacy of the model. Generally, optimum plans tend to be highly sensitive to model specification errors and

thus are suitable only if the degradation model is correct. Also, planning values that are appreciably in error may result in test plans that are far from optimum. It is highly desirable for a test plan to be robust (i.e., the plan should give useful results even if the assumed model and planning values are inaccurate). A traditional plan with more factor level combinations tends to be robust, but it is less precise than an optimum plan. In general, a compromise plan will be more useful in practical applications. A compromise plan combines the advantages of optimum and traditional test plans.

6.3 Traditional and Optimized Compromise Plans for the Application

A traditional test plan for the Adhesive Bond B application is presented in Table 3. This plan has some baseline units at the beginning of the experiment and 12 other combinations using equally spaced levels of time and temperature, each with the same number of test units.

Table 3: Traditional ADDT Plan

Temperature	Weeks					Totals
°C	0	10	12	14	16	
—	4					4
50		7	7	7	7	28
60		7	7	7	7	28
70		7	7	7	7	28
Totals	4	21	21	21	21	88

To find compromise between the optimum and the traditional test plans, the number of factor level combinations for a compromise plan should be greater than the optimum plan but less than the traditional plan. As suggested by the traditional plan, a compromise plan for the Adhesive Bond B allocates some test units at the beginning of the experiment and some units at each of nine equally spaced factor level combinations. The nine combinations have three equally spaced time levels and three equally spaced temperature levels. We can not optimize the times for the compromise plan because the optimization would degenerate to a plan with all units (other than the baseline units) allocated to the temperatures at the longest test time. Also, we can not optimize allocations because the optimum allocations would degenerate to a 3-point optimum plan. Therefore, the compromise plan uses three time levels at 12, 14, and 16 weeks respectively and the highest temperature level at 70 °C, as in the traditional plan. The lowest temperature of the compromise plan is chosen to minimize the large sample approximate variance of the estimated 0.01 failure-time quantile, which

is similar to the optimum plan. The middle temperature is the mean of the other two temperature levels. After rounding in allocating the 88 test units, the compromise plan has 9 units at each of the nine equally spaced factor level combinations and 7 test units at the baseline. The optimum lowest temperature for the compromise ADDT plan is 54 °C and the middle temperature is 62 °C, as presented in Table 4.

Table 4: Compromise ADDT Plan

Temperature °C	Weeks 0	12	14	16	Totals
—	7				7
54		9	9	9	27
62		9	9	9	27
70		9	9	9	27
Totals	7	27	27	27	88

6.4 Comparison of ADDT Plans

As explained in Section 4.3, the purpose of the test is to estimate t_p, the p quantile of the failure-time distribution. Denote the ML estimate of t_p by $\widehat{t}_p$. An approximate $100(1-\alpha)\%$ confidence interval for $\log(t_p)$ is

$$\log(\widehat{t}_p) \pm z_{(1-\alpha/2)}\sqrt{\widehat{\mathrm{Var}}\left[\log(\widehat{t}_p)\right]} = \log(\widehat{t}_p) \pm \log(\widehat{R}).$$

Exponentiation yields an approximate confidence interval for t_p

$$[\widehat{t}_p/\widehat{R},\ \widehat{t}_p\widehat{R}]$$

where

$$\widehat{R} = \exp\left[z_{(1-\alpha/2)}\sqrt{\widehat{\mathrm{Var}}\left[\log(\widehat{t}_p)\right]}\ \right]. \tag{8}$$

The estimated variance $\widehat{\mathrm{Var}}\left[\log(\widehat{t}_p)\right]$ can be obtained from the local information matrix in the usual way (see, for example, Appendix B.3 of Meeker and Escobar 1998). We call $\widehat{R}$ the "observed precision factor." To estimate t_p precisely, the confidence interval for t_p should be as narrow as possible.

For test planning purposes, $\widehat{\text{Var}}\left[\log(\widehat{t_p})\right]$ in (8) is replaced with $\text{Avar}\left[\log(\widehat{t_p})\right]$, the large sample approximation for $\text{Var}\left[\log(\widehat{t_p})\right]$, in the evaluations. This gives the precision factor

$$R = \exp\left[z_{(1-\alpha/2)}\sqrt{\text{Avar}\left[\log(\widehat{t_p})\right]}\right]$$

which can be used in test planning because it is a function of the model and its parameters (planning values) and does not depend on the data. Because R is an increasing function of $\text{Avar}\left[\log(\widehat{t_p})\right]$, minimizing the R precision factor is equivalent to minimizing $\text{Avar}\left[\log(\widehat{t_p})\right]$ and approximately equivalent to minimizing $\text{Var}\left[\log(\widehat{t_p})\right]$. R is easier to interpret as a measure of precision for a positive parameter when compared with $\text{Avar}\left[\log(\widehat{t_p})\right]$, so we will use it for the comparisons among different ADDT plans. The upper (lower) endpoint of the confidence interval for t_p is approximately $100(R-1)\%$ larger (smaller) than the ML estimate $\widehat{t_p}$.

For the Adhesive Bond B application, Table 5 compares four ADDT plans: the optimum plan (in Table 2), the compromise plan (in Table 4), the original plan (in Table 1), and the traditional plan (in Table 3) in terms of the R precision factors for estimating the 0.01 failure-time quantile at normal use conditions of 25 °C.

Table 5: Comparison of the R precision factors of the approximate 95% confidence intervals for estimating $t_{0.01}$ and other properties among four ADDT plans.

ADDT Plan	Number of Factor Levels Combinations	Lowest Temperature °C at the Maximum Time	Precision Factor R
Optimum	3	54.764	1.910
Compromise	10	54	2.208
Original	16	50	2.465
Traditional	13	50	2.512

The optimum ADDT plan has the smallest R precision factor and provides the most precise estimate of $t_{0.01}$. The original test plan has a smaller R precision factor than the traditional plan. This is because the original plan has more factor level combinations spaced over the whole experimental region, which can give more information about the failure-time distribution. As expected, the R precision factor for the compromise plan is smaller than that for the traditional plan but larger than that for the optimum plan. We would recommend the compromise plan in Table 5 or a similar compromise plan.

7 Effect of Test Plan Changes

The precision of estimating a specified quantity depends on the constraints of the application, such as sample size, maximum accelerating variable level (temperature in the Adhesive Bond B application), maximum test time, etc. In this section, we evaluate the effects that changes in the sample size and the factor-level (time and temperature) constraints have on the R precision factors (for estimating the 0.01 failure-time quantile at the 25 °C use conditions) for the Adhesive Bond B experiment. We also conduct a sensitivity analysis to study the effect of misspecification of the planning information. For some of these analyses, we omit details for the original and tradational test plans when they would require extra space.

7.1 Effect of Sample Size Changes

As noted in Section 6.4,

$$R = \exp\left[z_{(1-\alpha/2)}\sqrt{\text{Avar}\left[\log(\widehat{t_p})\right]}\right].$$

The variance factor, defined as $n\text{Avar}\left[\log(\widehat{t_p})\right]$, depends on the actual values of the parameters but does not depend on the sample size n. Thus the R precision factor for any sample size can be predicted from large sample approximation theory once we know one such factor. Relative to the precision factor for a sample size of 88, the precision factor as a function of n can be written as

$$R_n = \exp\left[\sqrt{\frac{88}{n}} \times \log(R_{88})\right] = R_{88}^{\sqrt{88/n}}$$

where R_{88} is the precision factor with $n = 88$. Figure 6 shows the R precision factors as a function of n for the four ADDT plans.

7.2 Effect of Maximum Temperature and Time Changes

Table 6 presents the R precision factors that would be obtained from the optimum and compromise plans if we were to change the maximum temperature and maximum test time. Note that in the actual application, 80 °C is thought to be too high, but we want to show the potential improvement in precision if temperature could be increased. The results for the initial optimum and compromise plans are marked in bold. The compromise plans have a fixed lower time level at 12 weeks, a changing maximum time, and a third time level which is the halfway between 12 weeks and the maximum

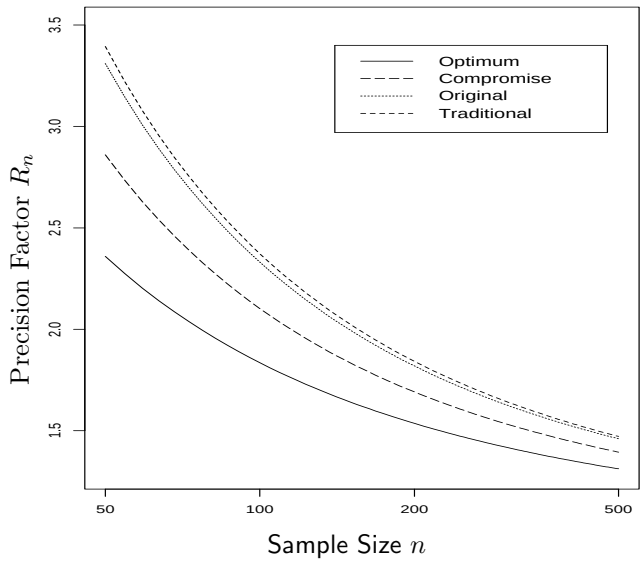

Figure 6: The R precision factors for estimating $t_{0.01}$ as a function of n for the four ADDT plans.

time.

Table 6: The R precision factors for estimating $t_{0.01}$ for optimum and compromise plans with changing maximum temperature and range of time.

Maximum Temperature °C	Maximum Weeks							
	Optimum Plan				Compromise Plan			
	14	16	18	20	14	16	18	20
60	3.004	2.780	2.610	2.475	4.266	3.957	3.690	3.463
70	2.003	**1.910**	1.837	1.778	2.302	**2.208**	2.127	2.057
80	1.559	1.519	1.487	1.466	1.642	1.612	1.588	1.568

As the maximum temperature or time increases, the observations are spread out so that the variance for the estimated failure-time quantile becomes smaller, which results in a decrease in the R precision factor.

7.3 Sensitivity to Misspecification of the Planning Information

Our method of assessing sensitivity to misspecification of the planning information follows the general approach used in Meeker (1984). From (2), the probability that an observational unit at the test

condition (τ, x) will fail is

$$\Phi\left[\frac{y_{\mathrm{f}} - \mu(\tau, x)}{\sigma}\right] = \Phi\left[\frac{h_d(\mathcal{D}_{\mathrm{f}}) - \beta_0 - \beta_1 \exp(\beta_2 x)\tau}{\sigma}\right]$$
$$= \Phi\left[\frac{h_d(\mathcal{D}_{\mathrm{f}}) - \beta_0}{\sigma} - \frac{\omega_{50}}{\sigma} \exp\left[\beta_2(x - x_{50})\right]\tau\right] \tag{9}$$

where, x_{50} is the transformed temperature of 50 °C, and ω_{50} is the degradation slope at 50 °C, as described in Section 4.1. Instead of being a function of the four parameters β_0, β_1, β_2 and σ, the probability in (9) only depends on the three standardized parameters $(h_d(\mathcal{D}_{\mathrm{f}}) - \beta_0)/\sigma$, ω_{50}/σ, β_2 and the two explanatory variables τ and x. This implies that n/σ^2 times the large sample approximate variance of the estimated failure-time quantile can be expressed in terms of these three standardized parameters. Using the standardized parameters makes it possible to do a general evaluations of the robustness of ADDT plans to misspecifications of the planning values by perturbing values in only three dimensions.

The idea of sensitivity analysis is to explore the effect of planning value misspecification across some plausible region of the parameter space. We chose nine sets of standardized parameter values in the parameter space (as shown in Tables 7 and 8) to evaluate the sensitivity of the test plans to misspecification of the planning information. The first set corresponds to the planning values given in Section 4.1 which were used for getting the optimum plan (6) for the application of interest. The other eight sets were chosen as the verticies of a cube in the parameter space that would not lead into nonsense degenerate optimized test plans.

For each set of actual parameter values, the optimum plan for estimating the 0.01 failure-time quantile was obtained. For comparison, another eight "optimum" plans were found for misspecification of ± 0.5 in $(h_d(\mathcal{D}_{\mathrm{f}}) - \beta_0)/\sigma$ and ± 0.2 in both ω_{50}/σ and β_2. Table 7 shows the worst and best ratios of the precision factors R for the "optimum" plans obtained with the misspecified values to the precision factor for the correct optimum plan. Similar comparisons for compromise plans are given in Table 8. Comparisons of the ratios in the two tables show that the compromise plans, when compared to the optimum plans, are much more robust to misspecified planning values.

Table 7: Effects of misspecifying $(h_d(\mathcal{D}_\mathrm{f}) - \beta_0)/\sigma$, ω_{50}/σ and β_2: worst and best precision factor ratios of the optimum plans for estimating the $p = 0.01$ failure-time quantile.

Actual Values			Misspecification of $(h_d(\mathcal{D}_\mathrm{f}) - \beta_0)/\sigma$ by ± 0.5 Misspecification of ω_{50}/σ and β_2 by ± 0.2							
				Deviation Yielding Worst Ratio				Deviation Yielding Best Ratio		
$\frac{h_d(\mathcal{D}_\mathrm{f})-\beta_0}{\sigma}$	$\frac{\omega_{50}}{\sigma}$	β_2	Worst Ratio	$\frac{h_d(\mathcal{D}_\mathrm{f})-\beta_0}{\sigma}$	$\frac{\omega_{50}}{\sigma}$	β_2	Best Ratio	$\frac{h_d(\mathcal{D}_\mathrm{f})-\beta_0}{\sigma}$	$\frac{\omega_{50}}{\sigma}$	β_2
−5	−0.65	0.6	1.20	+0.5	−0.2	−0.2	1.03	−0.5	−0.2	+0.2
−5	−0.5	0.5	1.31	+0.5	−0.2	−0.2	1.06	−0.5	−0.2	+0.2
−5	−0.5	0.6	1.19	+0.5	−0.2	−0.2	1.04	−0.5	−0.2	+0.2
−5	−0.6	0.5	1.30	+0.5	−0.2	−0.2	1.05	−0.5	−0.2	+0.2
−5	−0.6	0.6	1.19	+0.5	−0.2	−0.2	1.03	−0.5	−0.2	+0.2
−6	−0.5	0.5	1.23	+0.5	−0.2	−0.2	1.06	−0.5	−0.2	+0.2
−6	−0.5	0.6	1.14	+0.5	−0.2	−0.2	1.04	−0.5	−0.2	+0.2
−6	−0.6	0.5	1.20	+0.5	−0.2	−0.2	1.05	−0.5	−0.2	+0.2
−6	−0.6	0.6	1.12	+0.5	−0.2	−0.2	1.03	−0.5	−0.2	+0.2

Table 8: Effects of misspecifying $(h_d(\mathcal{D}_\mathrm{f}) - \beta_0)/\sigma$, ω_{50}/σ and β_2: worst and best precision factor ratios of the compromise plans for estimating the $p = 0.01$ failure-time quantile.

Actual Values			Misspecification of $(h_d(\mathcal{D}_\mathrm{f}) - \beta_0)/\sigma$ by ± 0.5 Misspecification of ω_{50}/σ and β_2 by ± 0.2							
				Deviation Yielding Worst Ratio				Deviation Yielding Best Ratio		
$\frac{h_d(\mathcal{D}_\mathrm{f})-\beta_0}{\sigma}$	$\frac{\omega_{50}}{\sigma}$	β_2	Worst Ratio	$\frac{h_d(\mathcal{D}_\mathrm{f})-\beta_0}{\sigma}$	$\frac{\omega_{50}}{\sigma}$	β_2	Best Ratio	$\frac{h_d(\mathcal{D}_\mathrm{f})-\beta_0}{\sigma}$	$\frac{\omega_{50}}{\sigma}$	β_2
−5	−0.65	0.6	1.08	+0.5	−0.2	−0.2	1.00	+0.5	−0.2	+0.2
−5	−0.5	0.5	1.13	+0.5	−0.2	−0.2	1.01	+0.5	−0.2	+0.2
−5	−0.5	0.6	1.09	+0.5	−0.2	−0.2	1.00	+0.5	−0.2	+0.2
−5	−0.6	0.5	1.12	+0.5	−0.2	−0.2	1.00	+0.5	−0.2	+0.2
−5	−0.6	0.6	1.08	+0.5	−0.2	−0.2	1.00	+0.5	−0.2	+0.2
−6	−0.5	0.5	1.10	+0.5	−0.2	−0.2	1.02	+0.5	−0.2	+0.2
−6	−0.5	0.6	1.07	+0.5	−0.2	−0.2	1.01	+0.5	−0.2	+0.2
−6	−0.6	0.5	1.09	+0.5	−0.2	−0.2	1.02	+0.5	−0.2	+0.2
−6	−0.6	0.6	1.06	+0.5	−0.2	−0.2	1.01	+0.5	−0.2	+0.2

8 Monte Carlo Simulation to Evaluate Test Plans

Monte Carlo simulation is a powerful tool to provide visualization of the results that might be obtained from a given test plan, and to check the large sample approximations used to evaluate and optimize ADDT plans.

Simulation and analytical evaluation, based on the large sample approximations, are complementary tools for test planning. Simulation is best suited for exact evaluation of test plans and for providing useful insight through visualization of sampling variability in the parameter estimates. Simulation also provides a check on the adequacy of the large sample approximations. The large sample approximations are, however, important for doing computations quickly, as is needed in optimization or comparing a large number of different alternative test plans to assess sample size needs. Generally it takes orders of magnitude more computer time to evaluate a plan with simulation relative to the use of a large sample approximation.

For each test plan in Table 5, a simulation trial consists of a set of 88 observations obtained according to the test plan, the given model, and the planning information. The simulated data are used to obtain the maximum likelihood estimates of the parameters, the estimate of the covariance matrix for the ML estimates, and the observed precision factor of an approximate 95% confidence interval for estimating $t_{0.01}$. The simulation was repeated 1000 times for each test plan.

Figure 7 shows estimates of the 0.01 failure-time quantile versus temperature for the first 50 realizations of the simulation for each test plan. The longer lines represent the values computed from the planning values, which we call the "true" values. The geometric mean and the 0.9 quantile of the 1000 observed precision factors $\widehat{R}$, denoted by $\bar{R}$ and $R_{0.90}$ respectively, are given in the figure caption for each plan.

The $\bar{R}$ values tend to be close to the R values obtained from the large sample approximations given in Table 5. The optimum plan has the narrowest group of simulated lines. The spread of the group of simulated lines for the compromise plan is wider than that for the optimum plan but narrower than that for the traditional plan or for the original plan. This is consistent with our previous comments about the estimation precision of different test plans, based on the R precision factors. We have studied the distribution of $\widehat{R}$ for all of the test plans in Table 5. The distributions are similar although there tends to be less spread in the distribution with the optimum plan and more spread with the traditional plan. This is not surprising given that the variability in $\widehat{R}$ is related to the variability of the ML estimators of the model parameters.

To assess the effectiveness of the test plan to estimate the 0.01 failure-time quantile at 25 °C, the 1000 simulated estimates of $t_{0.01}$ for the compromise plan are depicted in Figure 8. The geometric mean of these estimates is 775.01 weeks, relative to the "true" value of $t_{0.01} = 755.48$ weeks from the planning values. The distribution of the $t_{0.01}$ values is skewed to the right. Although the probability

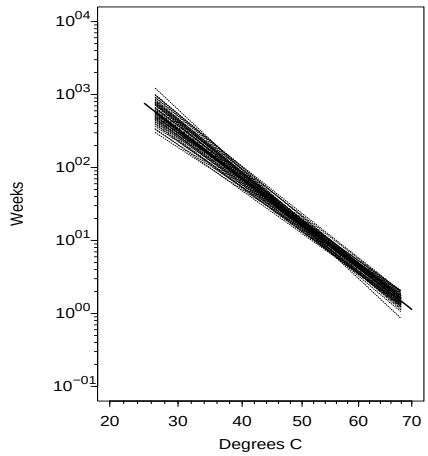

(a) Optimum Plan
$\bar{R} = 1.795, R_{0.90} = 1.923$

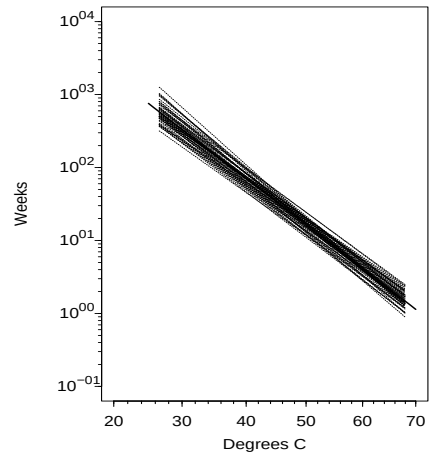

(b) Compromise Plan
$\bar{R} = 2.092, R_{0.90} = 2.361$

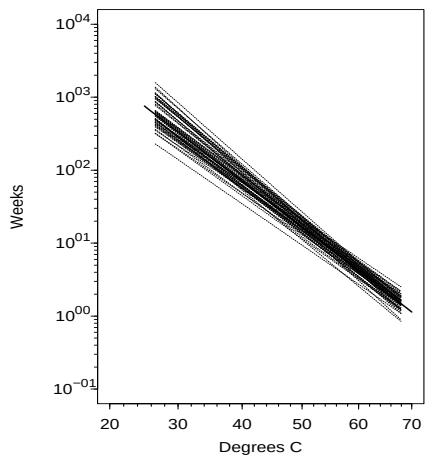

(c) Original Plan
$\bar{R} = 2.353, R_{0.90} = 2.748$

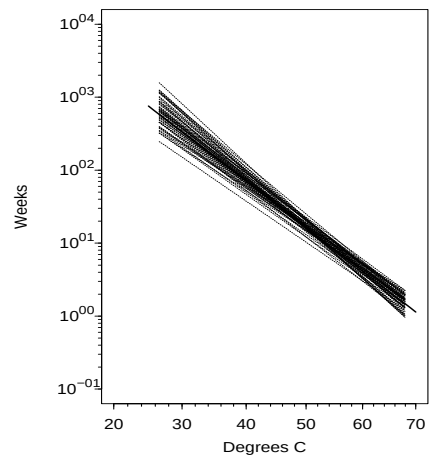

(d) Traditional Plan
$\bar{R} = 2.414, R_{0.90} = 2.888$

Figure 7: Simulation of 0.01 failure-time quantile estimates versus temperature for the optimum plan, the compromise plan, the original plan, and the traditional plan.

is small (estimated to be about 0.019 from the simulation results), if the planning values were correct, it would be possible that one could get an estimate of $t_{0.01}$ exceeding 2000 weeks.

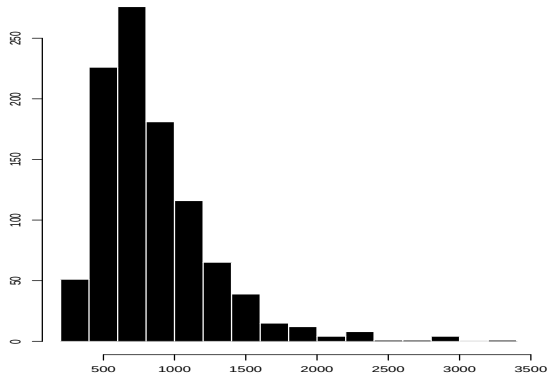

Figure 8: Histogram of the simulated estimates of 0.01 failure-time quantile for the compromise plan.

9 Conclusions and Extensions

Accelerated destructive degradation testing is an important tool for making reliability inferences and predictions, especially when test time is limited and few or no failures are expected at lower levels of the accelerating variables. The methodology presented in this paper can be extended in several important directions, suggesting areas for future research. These include the following:

1. For some products, there may be more than one failure mechanism. This can cause observations to be right censored. For such observations, the strength is unknown and is greater than the censoring value.

2. A model with multiple accelerating variables (e.g., temperature and humidity) could be developed.

3. As explained in Section 2.1, the relationship between the mean transformed degradation path and the transformed time is linear at a fixed accelerating variable level. The work in this paper can be extended to the degradation models that have a nonlinear relationship.

4. While the basic ideas and numerical methods in this paper hold for any log-location-scale distribution, the results in the appendix are for the normal distribution as in our example. It may be possible to derive similar results in general for other log-location-scale distributions, but it will be more difficult when the information matrix is not block diagonal.

5. For some applications, prior knowledge about the failure mechanism might provide information about some model parameters that could be useful to improve the precision of estimating specified quantities. Bayesian methods could be used in such situations.

6. If one is going to use prior information in the estimation of model parameters, then generally, it is important that prior information should also be used in test planning. It would be useful to apply methods like those described in Zhang and Meeker (2006) for ADDT planning.

Acknowledgments

We would like to thank a referee, the associate editor, and the editor who made useful comments that helped us improve our paper.

A Appendix

A.1 ADDT Model Large Sample Approximate Covariance Matrix

Let $\widehat{\boldsymbol{\theta}}$ be the ML estimate of $\boldsymbol{\theta} = (\beta_0, \beta_1, \beta_2, \sigma)'$ based on n observations. Under the usual regularity conditions (for example, see Appendix B.4 of Meeker and Escobar 1998), the following results hold for large samples.

- $\widehat{\boldsymbol{\theta}} \dot{\sim} \text{MVN}(\boldsymbol{\theta}, \Sigma_{\widehat{\boldsymbol{\theta}}})$, where $\Sigma_{\widehat{\boldsymbol{\theta}}} = I_{\boldsymbol{\theta}}^{-1}$, and the Fisher information matrix I_θ with r test conditions is

$$I_\theta = \text{E}\left[-\frac{\partial^2 \mathcal{L}}{\partial \boldsymbol{\theta} \partial \boldsymbol{\theta}'}\right] = n \sum_{i=1}^{r} \pi_i \text{E}\left[-\frac{\partial^2 \mathcal{L}_i}{\partial \boldsymbol{\theta} \partial \boldsymbol{\theta}'}\right] = n \sum_{i=1}^{r} \pi_i I_i. \tag{10}$$

  $\mathcal{L}_i = \log[L_i(\boldsymbol{\theta})]$ is the contribution of a single observation at test condition $\boldsymbol{v}_i = (\tau_i, x_i)$ to the log-likelihood, and $L_i(\boldsymbol{\theta}) = \frac{1}{\sigma}\,\phi\,[(Y_i - \mu_i)/\sigma]$. $\text{E}(\bullet)$ is the expectation operator and the expectation is with respect to the data to be collected in the ADDT. I_i is the contribution of one observation at $\boldsymbol{v}_i$ to I_θ. Let $\mathcal{I}(\boldsymbol{\xi})$ denote the large sample scaled Fisher matrix for a particular test plan $\boldsymbol{\xi}$, then $\mathcal{I}(\boldsymbol{\xi}) = \frac{1}{n} I_\theta$ (see B.3 of Meeker and Escobar 1998).

- For a scalar $\widehat{g} = g(\widehat{\boldsymbol{\theta}}) \dot{\sim} \text{NOR}[g(\boldsymbol{\theta}), \text{Avar}(\widehat{g})]$, the delta method gives

$$\text{Avar}(\widehat{g}) = \left[\frac{\partial g(\boldsymbol{\theta})}{\partial \boldsymbol{\theta}}\right]' \Sigma_{\widehat{\boldsymbol{\theta}}} \left[\frac{\partial g(\boldsymbol{\theta})}{\partial \boldsymbol{\theta}}\right],$$

  allowing us to compute the large sample approximate variance for a desired function of $\boldsymbol{\theta}$.

A.2 ADDT Model Fisher Information Matrix

The contribution I_i to the Fisher information matrix (10) in terms of parameters $\boldsymbol{\theta}$ is

$$I_i = \frac{1}{\sigma^2} \begin{bmatrix} f_{11}(\zeta)\boldsymbol{u}_i\boldsymbol{u}_i' & f_{12}(\zeta)\boldsymbol{u}_i \\ f_{12}(\zeta)\boldsymbol{u}_i & f_{22}(\zeta) \end{bmatrix}$$

where $f_{11}(\zeta)$, $f_{12}(\zeta)$, $f_{22}(\zeta)$ elements can be computed using the LSINF algorithm (see Escobar and Meeker 1994). In a situation where there is censoring, ζ depends on the test conditions. For the normal distribution and no censoring, it can be shown that $f_{11} = 1, f_{12} = 0,$ and $f_{22} = 2$. $\boldsymbol{u}_i$ is the vector of partial derivatives of the degradation with respect to the $\boldsymbol{\beta}$ parameters. That is

$$\boldsymbol{u}_i = \begin{bmatrix} \dfrac{\partial \mu_i}{\partial \beta_0} \\ \dfrac{\partial \mu_i}{\partial \beta_1} \\ \dfrac{\partial \mu_i}{\partial \beta_2} \end{bmatrix} = \begin{bmatrix} 1 \\ \exp(\beta_2 x_i)\tau_i \\ \beta_1\, x_i\, \exp(\beta_2 x_i)\tau_i \end{bmatrix}$$

where $\mu_i = \beta_0 + \beta_1 \exp(\beta_2 x_i)\tau_i$, $\tau_i = h_t(t_i)$, and $x_i = h_a(\text{AccVar}_i)$. For ADDT planning, the Fisher information matrix is evaluated at planning values $\boldsymbol{\theta}^{\square}$.

A.3 Large Sample Approximate Variance of $h_t(\widehat{t_p})$ and $\widehat{t_p}$

We can write $\text{Avar}[h_t(\widehat{t_p})]$ as a function of $\Sigma_{\widehat{\boldsymbol{\theta}}}$. Define $\boldsymbol{c} = \partial h_t(t_p)/\partial \boldsymbol{\theta}$. Then direct computations yield

$$\text{Avar}[h_t(\widehat{t_p})] = \boldsymbol{c}'\Sigma_{\widehat{\boldsymbol{\theta}}}\boldsymbol{c} = \boldsymbol{c}' I_{\boldsymbol{\theta}}^{-1}\boldsymbol{c} = \frac{1}{n}\boldsymbol{c}' \left[\mathcal{I}(\boldsymbol{\xi})\right]^{-1} \boldsymbol{c}. \tag{11}$$

For decreasing degradation, $h_t(t_p) = \nu + \varsigma\Phi^{-1}(p)$ for $p \geq \Phi\left(-\nu/\varsigma\right)$. The elements of $\boldsymbol{c}$ are:

$$\begin{aligned}
\frac{\partial h_t(t_p)}{\partial \beta_0} &= -\frac{1}{\beta_1 \exp(\beta_2 x)} & \frac{\partial h_t(t_p)}{\partial \beta_1} &= -\frac{h_t(t_p)}{\beta_1} \\
\frac{\partial h_t(t_p)}{\partial \beta_2} &= -x\, h_t(t_p) & \frac{\partial h_t(t_p)}{\partial \sigma} &= -\frac{\Phi^{-1}(p)}{\beta_1 \exp(\beta_2 x)}
\end{aligned}$$

For increasing degradation, $h_t(t_p) = -\left[\nu + \varsigma\Phi^{-1}(1-p)\right]$ for $p \geq 1 - \Phi\left(-\nu/\varsigma\right)$. The elements of $\boldsymbol{c}$ are the same as those for decreasing degradation expect for

$$\frac{\partial h_t(t_p)}{\partial \sigma} = -\frac{\Phi^{-1}(1-p)}{\beta_1 \exp(\beta_2 x)}.$$

Using the delta method,

$$\mathrm{Avar}(\widehat{t_p}) = \left(\left. \frac{\partial h_t^{-1}(z)}{\partial z} \right|_{h_t(t_p^{\square})} \right)^2 \mathrm{Avar}[h_t(\widehat{t_p})].$$

B Appendix

B.1 General Equivalence Theorem

The following results apply to the ADDT planning problem:

1. The objective function $\Psi\left[\mathcal{I}(\boldsymbol{\xi})\right]$ defined in (4) is strictly concave. That is, if $0 < \alpha < 1$ and $\boldsymbol{\xi}$, $\boldsymbol{\eta}$ are two test plans ($\boldsymbol{\xi} \neq \boldsymbol{\eta}$) then

$$\Psi\left[\alpha\mathcal{I}(\boldsymbol{\xi}) + (1-\alpha)\mathcal{I}(\boldsymbol{\eta})\right] > \alpha\Psi[\mathcal{I}(\boldsymbol{\xi})] + (1-\alpha)\Psi[\mathcal{I}(\boldsymbol{\eta})]. \tag{12}$$

2. The directional derivative, Λ, of Ψ at $\boldsymbol{\xi}$ and in the direction of an alternative plan $\boldsymbol{\eta}$ is

$$\Lambda(\boldsymbol{\xi}, \boldsymbol{\eta}) = \boldsymbol{c}\,'[\mathcal{I}(\boldsymbol{\xi})]^{-1}\mathcal{I}(\boldsymbol{\eta})[\mathcal{I}(\boldsymbol{\xi})]^{-1}\,\boldsymbol{c} - \boldsymbol{c}\,'\,[\mathcal{I}(\boldsymbol{\xi})]^{-1}\,\boldsymbol{c} \tag{13}$$

   where $\boldsymbol{c}$, $\mathcal{I}(\boldsymbol{\xi})$, and $\mathcal{I}(\boldsymbol{\eta})$ are evaluated at the planning values.

3. For fixed $\boldsymbol{\xi}$, the directional derivative $\Lambda(\boldsymbol{\xi}, \boldsymbol{\eta})$ is linear in $\boldsymbol{\eta}$ in the following sense (Whittle

1973, equation 7). For $a_i \geq 0, \sum_i a_i = 1$

$$\Lambda\left(\boldsymbol{\xi}, \sum_i a_i \boldsymbol{\eta}_i\right) = \sum_i a_i \Lambda(\boldsymbol{\xi}, \boldsymbol{\eta}_i)$$

where the $\boldsymbol{\eta}_i$s are alternative test plans. That is, for an alternative test plan specified by the convex combination $\sum_i a_i \boldsymbol{\eta}_i$, the directional derivative is the corresponding convex combination of the $\Lambda(\boldsymbol{\xi}, \boldsymbol{\eta}_i)$.

4. Consider the directional derivative $\Lambda(\boldsymbol{\xi}, \boldsymbol{\xi}_{\boldsymbol{v}})$ in the direction of the plan that puts all units at $\boldsymbol{v}$. Then the plan $\boldsymbol{\xi}^*$ is optimal if and only if $\sup_{\boldsymbol{v}} \Lambda(\boldsymbol{\xi}^*, \boldsymbol{\xi}_{\boldsymbol{v}}) = 0$.

5. The test conditions $\boldsymbol{v}_i^*$ in the optimal plan are a subset of the conditions $\boldsymbol{v}$ satisfying $\Lambda(\boldsymbol{\xi}^*, \boldsymbol{\xi}_{\boldsymbol{v}}) = 0$.

Proof of Results

To prove (12), the concavity of the objective function, use (4) to get

$$\begin{aligned}
&\Psi\left[\alpha\mathcal{I}(\boldsymbol{\xi}) + (1-\alpha)\mathcal{I}(\boldsymbol{\eta})\right] - \alpha\Psi[\mathcal{I}(\boldsymbol{\xi})] - (1-\alpha)\Psi[\mathcal{I}(\boldsymbol{\eta})] \\
&= \boldsymbol{c}'\left\{\alpha[\mathcal{I}(\boldsymbol{\xi})]^{-1} + (1-\alpha)[\mathcal{I}(\boldsymbol{\eta})]^{-1} - [\alpha\mathcal{I}(\boldsymbol{\xi}) + (1-\alpha)\mathcal{I}(\boldsymbol{\eta})]^{-1}\right\}\boldsymbol{c} > 0
\end{aligned}$$

where the inequality on the right hand side of the last equation follows from the fact that the matrix $\alpha[\mathcal{I}(\boldsymbol{\xi})]^{-1} + (1-\alpha)[\mathcal{I}(\boldsymbol{\eta})]^{-1} - [\alpha\mathcal{I}(\boldsymbol{\xi}) + (1-\alpha)\mathcal{I}(\boldsymbol{\eta})]^{-1}$ is positive definite; see Moore (1973).

To prove (13), start with the definition

$$\Lambda(\boldsymbol{\xi}, \boldsymbol{\eta}) = \lim_{\delta \to 0^+} \frac{\Psi[(1-\delta)\boldsymbol{\xi} + \delta\boldsymbol{\eta}] - \Psi(\boldsymbol{\xi})}{\delta}. \tag{14}$$

From (14), using l'Hôpital's rule for limits, the chain rule for derivatives, and

$$\frac{\partial\Psi(\boldsymbol{\xi})}{\partial\boldsymbol{\xi}} = [\mathcal{I}(\boldsymbol{\xi})]^{-1}\boldsymbol{c}\boldsymbol{c}'[\mathcal{I}(\boldsymbol{\xi})]^{-1}$$

one gets

$$\Lambda(\boldsymbol{\xi}, \boldsymbol{\eta}) = -\mathrm{tr}\left[\mathcal{I}(\boldsymbol{\xi})\frac{\partial\Psi(\boldsymbol{\xi})}{\partial\boldsymbol{\xi}}\right] + \mathrm{tr}\left[\mathcal{I}(\boldsymbol{\eta})\frac{\partial\Psi(\boldsymbol{\xi})}{\partial\boldsymbol{\xi}}\right] = \boldsymbol{c}'[\mathcal{I}(\boldsymbol{\xi})]^{-1}\mathcal{I}(\boldsymbol{\eta})[\mathcal{I}(\boldsymbol{\xi})]^{-1}\boldsymbol{c} - \boldsymbol{c}'[\mathcal{I}(\boldsymbol{\xi})]^{-1}\boldsymbol{c}. \tag{15}$$

To show the linearity of $\Lambda(\boldsymbol{\xi}, \boldsymbol{\eta})$ with respect to $\boldsymbol{\eta}$, use (15) to write

$$\Lambda\left(\boldsymbol{\xi}, \sum_i a_i \boldsymbol{\eta}_i\right) = \boldsymbol{c}'[\mathcal{I}(\boldsymbol{\xi})]^{-1}\mathcal{I}\left(\sum_i a_i \boldsymbol{\eta}_i\right)[\mathcal{I}(\boldsymbol{\xi})]^{-1}\boldsymbol{c} - \boldsymbol{c}'[\mathcal{I}(\boldsymbol{\xi})]^{-1}\boldsymbol{c}. \tag{16}$$

Using the fact that $\mathcal{I}\left(\sum_i a_i \boldsymbol{\eta}_i\right) = \sum_i a_i \mathcal{I}(\boldsymbol{\eta}_i)$, expanding the first term on the right hand side of (16), and after some simplications, one obtains $\Lambda\left(\boldsymbol{\xi}, \sum_i a_i \boldsymbol{\eta}_i\right) = \sum_i a_i \Lambda(\boldsymbol{\xi}, \boldsymbol{\eta}_i)$.

Because the objective function $\Psi[\mathcal{I}(\boldsymbol{\xi})]$ is concave and its directional derivative $\Lambda(\boldsymbol{\xi}, \boldsymbol{\eta})$ is linear in $\boldsymbol{\eta}$, Results 4 and 5 follow immediately from *Theorem 1* parts (i), (ii), (iii), and (c) in Whittle (1973, page 125).

B.2 Alternative Optimum Plans

This section shows an alternative plan $\boldsymbol{\xi}^a$ in (7) is optimum. The information matrix for the optimal plan $\boldsymbol{\xi}^*$ given in equation (5) is

$$\begin{aligned}\mathcal{I}(\boldsymbol{\xi}^*) &= \pi_1^*\mathcal{I}(\boldsymbol{v}_1^*) + \pi_2^*\mathcal{I}(\boldsymbol{v}_2^*) + \pi_3^*\mathcal{I}(\boldsymbol{v}_3^*) \\ &= \pi_1^*\begin{bmatrix} 1 & \mathbf{0}' & 0 \\ \mathbf{0} & \mathbf{0}\mathbf{0}' & \mathbf{0} \\ 0 & \mathbf{0}' & 2 \end{bmatrix} + \pi_2^*\begin{bmatrix} 1 & \tau_M \boldsymbol{e}_2^{*\prime} & 0 \\ \tau_M \boldsymbol{e}_2^* & \tau_M^2 \boldsymbol{e}_2^*\boldsymbol{e}_2^{*\prime} & \mathbf{0} \\ 0 & \mathbf{0}' & 2 \end{bmatrix} + \pi_3^*\begin{bmatrix} 1 & \tau_M \boldsymbol{e}_3^{*\prime} & 0 \\ \tau_M \boldsymbol{e}_3^* & \tau_M^2 \boldsymbol{e}_3^*\boldsymbol{e}_3^{*\prime} & \mathbf{0} \\ 0 & \mathbf{0}' & 2 \end{bmatrix}\end{aligned} \tag{17}$$

where $\boldsymbol{e}_2^* = [\exp(\beta_2 x_2^*),\ \beta_1 x_2^* \exp(\beta_2 x_2^*)]'$ and $\boldsymbol{e}_3^* = [\exp(\beta_2 x_3^*),\ \beta_1 x_3^* \exp(\beta_2 x_3^*)]'$.

For the alternative plan $\boldsymbol{\xi}^a$, $\pi_3 = \pi_3^*$, $\pi_2 = \pi_2^*\tau_M/\tau_a$, and $\pi_1 = \pi_1^* + \pi_2^* - \pi_2^*\tau_M/\tau_a$, then after some simplifications, one obtains $\mathcal{I}(\boldsymbol{\xi}^a) = \mathcal{I}(\boldsymbol{\xi}^*) - m_0\boldsymbol{u}_2^*\boldsymbol{u}_2^{*\prime}$, where $m_0 = \pi_2^*(\tau_M^2 - \tau_M\tau_a)$ and $\boldsymbol{u}_2^{*\prime} = (0, \boldsymbol{e}_2^{*\prime}, 0)$. Consequently, using a result to compute the inverse of a sum of matrices (see Problem 2.8 on page 33 of Rao, 1973), one gets

$$\begin{aligned}\boldsymbol{c}'\left[\mathcal{I}(\boldsymbol{\xi}^a)\right]^{-1}\boldsymbol{c} &= \boldsymbol{c}'\left[\mathcal{I}(\boldsymbol{\xi}^*) - m_0\boldsymbol{u}_2^*\boldsymbol{u}_2^{*\prime}\right]^{-1}\boldsymbol{c} \\ &= \boldsymbol{c}'\left[\mathcal{I}(\boldsymbol{\xi}^*)\right]^{-1}\boldsymbol{c} + \frac{m_0\boldsymbol{c}'\left[\mathcal{I}(\boldsymbol{\xi}^*)\right]^{-1}\boldsymbol{u}_2^*\boldsymbol{u}_2^{*\prime}\left[\mathcal{I}(\boldsymbol{\xi}^*)\right]^{-1}\boldsymbol{c}}{1 - m_0\boldsymbol{u}_2^{*\prime}\left[\mathcal{I}(\boldsymbol{\xi}^*)\right]^{-1}\boldsymbol{u}_2^*} = \boldsymbol{c}'\left[\mathcal{I}(\boldsymbol{\xi}^*)\right]^{-1}\boldsymbol{c}.\end{aligned} \tag{18}$$

The last step in obtaining (18) above follows from the fact that $\boldsymbol{c}'\left[\mathcal{I}(\boldsymbol{\xi}^*)\right]^{-1}\boldsymbol{u}_2^* = 0$ (see details below). Equation (18) shows that the alternative plan $\boldsymbol{\xi}^a$ is optimum.

Now we prove that $\boldsymbol{c}'\left[\mathcal{I}(\boldsymbol{\xi}^*)\right]^{-1}\boldsymbol{u}_2^* = 0$. First we derive a simple general expression for the direc-

tional derivatives. Consider the test plan $\boldsymbol{\xi}_{\boldsymbol{v}}$ with $\boldsymbol{v} = (\tau, x)$. Define $\boldsymbol{e} = [\exp(\beta_2 x), \beta_1 x \exp(\beta_2 x)]'$. Then using the fact that $\Lambda(\boldsymbol{\xi}^*, \boldsymbol{\xi}_{\boldsymbol{v}_1^*}) = 0$ (recall that $\boldsymbol{v}_1^*$ is a test condition in the optimum plan), after simple manipulations, one gets

$$\Lambda(\boldsymbol{\xi}^*, \boldsymbol{\xi}_{\boldsymbol{v}}) = \tau \boldsymbol{c}' \left[\mathcal{I}(\boldsymbol{\xi}^*)\right]^{-1} \begin{bmatrix} 0 & \boldsymbol{e}' & 0 \\ \boldsymbol{e} & \tau \boldsymbol{e}\boldsymbol{e}' & \boldsymbol{0} \\ 0 & \boldsymbol{0}' & 0 \end{bmatrix} \left[\mathcal{I}(\boldsymbol{\xi}^*)\right]^{-1} \boldsymbol{c} = \tau \boldsymbol{r}_2' \boldsymbol{e} \left(2r_1 + \tau \boldsymbol{r}_2' \boldsymbol{e}\right) \tag{19}$$

where r_1 is a scalar and $\boldsymbol{r}_2$ is a vector with two components defined by $(r_1, \boldsymbol{r}_2', r_3) = \boldsymbol{c}' \left[\mathcal{I}(\boldsymbol{\xi}^*)\right]^{-1}$. Because $\boldsymbol{\xi}^*$ is optimum, $\Lambda(\boldsymbol{\xi}^*, \boldsymbol{\xi}_{\boldsymbol{v}_1^*}) = \Lambda(\boldsymbol{\xi}^*, \boldsymbol{\xi}_{\boldsymbol{v}_2^*}) = \Lambda(\boldsymbol{\xi}^*, \boldsymbol{\xi}_{\boldsymbol{v}_3^*}) = 0$. Then in view of (19)

$$\boldsymbol{r}_2' \boldsymbol{e}_2^* (2r_1 + \tau_M \boldsymbol{r}_2' \boldsymbol{e}_2^*) = 0 \tag{20}$$

$$\boldsymbol{r}_2' \boldsymbol{e}_3^* (2r_1 + \tau_M \boldsymbol{r}_2' \boldsymbol{e}_3^*) = 0. \tag{21}$$

Because x_3^* is optimum, the directional derivative function must have a relative maximum at that point. Then

$$\frac{\partial \Lambda(\boldsymbol{\xi}^*, \boldsymbol{\xi}_{\boldsymbol{v}})}{\partial x} = 2\tau_M \left(r_1 + \tau_M \boldsymbol{r}_2' \boldsymbol{e}_3^*\right) \left(\boldsymbol{r}_2' \frac{\partial \boldsymbol{e}}{\partial x}\right)\Bigg|_{x_3^*} = 0. \tag{22}$$

Equations (20), (21), and (22) imply $\boldsymbol{r}_2' \boldsymbol{e}_2^* = 0, \boldsymbol{r}_2' \boldsymbol{e}_3^* = -r_1/2,$ and $\boldsymbol{r}_2' \partial \boldsymbol{e} / \partial x|_{x_3^*} = 0$. Consequently, $\boldsymbol{c}' \left[\mathcal{I}(\boldsymbol{\xi}^*)\right]^{-1} \boldsymbol{u}_2^* = 0$ as required.

References

[1] Boulanger, M., and Escobar, L. A. (1994), "Experimental Design for a Class of Accelerated Degradation Tests," *Technometrics*, **36**, 260–272.

[2] Escobar, L. A., and Meeker, W. Q. (1994), "Fisher Information Matrix for the Extreme Value, Normal, and Logistic Distributions and Censored Data," *Applied Statistics*, **43**, 533–540.

[3] Escobar, L. A., and Meeker, W. Q. (1995), "Planning Accelerated Life Tests With Two or More Experimental Factors," *Technometrics*, **37**, 411–427.

[4] Escobar, L. A., Meeker, W. Q., Kugler, D. L., and Kramer, L. L. (2003), "Accelerated Destructive Degradation Tests: Data, Models, and Analysis," Chapter 21 in *Mathematical and Statistical Methods in Reliability*, B. H. Lindqvist and K. A. Doksum, Editors, River Edge, NJ: World Scientific Publishing Company.

[5] Moore, M. H. (1973), "A Convex Matrix Function," *American Mathematical Monthly*, **80**, 408–409.

[6] Meeker, W. Q. (1984), "A Comparison of Accelerated Life Test Plans for Weibull and Lognormal Distributions and Type I Censoring," *Technometrics*, **26**, 157–171.

[7] Meeker, W. Q., and Escobar, L. A. (1998), *Statistical Methods for Reliability Data*, New York: John Wiley & Sons.

[8] Nelson, W. (1981), "Analysis of Performance Degradation Data From Accelerated Tests," *IEEE Transactions on Reliability*, **R-30**, 149–155.

[9] Nelson, W. (1990), *Accelerated Testing: Statistical Models, Test Plans, and Data Analyses*, New York: John Wiley & Sons.

[10] Nelson, W. (2005a), "A Bibliography of Accelerated Test Plans," *IEEE Transactions on Reliability*, **54**, 194–197.

[11] Nelson, W. (2005b), "A Bibliography of Accelerated Test Plans Part II - References," *IEEE Transactions on Reliability*, **54**, 370–373.

[12] Pukelsheim, F. (1993), *Optimal Design of Experiments*, New York: John Wiley & Sons.

[13] Rao, C. R. (1973), *Linear Statistical Inference and its Applications*, New York: John Wiley & Sons.

[14] Zhang, Y., and Meeker, W. Q. (2006), "Bayesian Methods for Planning Accelerated Life Tests," *Technometrics*, **48**, 49–60.

[15] Whittle, P. (1973), "Some General Points in the Theory of Optimal Experimental Design," *Journal of the Royal Statistical Society*, Ser. B, **35**, 123–130.